Dimeric Phenalenyl-Based Neutral Radical Molecular Conductors

X. Chi,[†] M. E. Itkis,[†] K. Kirschbaum,[‡] A. A. Pinkerton,[‡] R. T. Oakley,[§] A. W. Cordes,[||] and R. C. Haddon[†,*]

Contribution from the Departments of Chemistry and Physics, Advanced Carbon Materials Center, University of Kentucky, Lexington, Kentucky 40506-0055, Department of Chemistry, University of Toledo, Toledo, Ohio 43606-3390, Department of Chemistry, University of Waterloo, Waterloo, Ontario N2L 3G1, Canada, and Department of Chemistry and Biochemistry, University of Arkansas, Fayetteville, Arkansas 72701

Received November 15, 2000

Abstract: We report the preparation, crystallization, and solid-state characterization of ethyl (**3**)- and butyl (**4**)-substituted spiro-biphenalenyl radicals. Both of these compounds are found to be conducting face-to-face π-dimers in the solid state but with different room-temperature magnetic ground states. At room temperature, **4** exists as a diamagnetic π-dimer (interplanar separation of ~3.1 Å), whereas **3** is a paramagnetic π-dimer (interplanar separation of ~3.3 Å), and both compounds show phase transitions between the paramagnetic and diamagnetic forms. Electrical resistivity measurements of single crystals of **3** and **4** show that the transition from the high-temperature paramagnetic π-dimer form to the low-temperature diamagnetic π-dimer structure is accompanied by an increase in conductivity by about 2 orders of magnitude. This behavior is unprecedented and is very difficult to reconcile with the usual understanding of a Peierls dimerization, which inevitably leads to an insulating ground state. We tentatively assign the enhancement in the conductivity to a decrease in the on-site Coulombic correlation energy (*U*), as the dimers form a super-molecule with twice the amount of conjugation.

Introduction

For some time we have attempted to prepare an intrinsic molecular metal, that is, a solid composed of a single molecular species that would function as a classical (mono)atomic metal and superconductor.[1,2] This necessarily requires the crystallization of a neutral radical, and we have argued in favor of the phenalenyl system.[3,4] We have recently reported the first phenalenyl-based neutral radical conductor (**1**).[5] Although the solid is composed of isolated molecules (no contacts within van der Waals separation), this compound exhibits the highest conductivity of any neutral organic molecule (cf. ref 6).

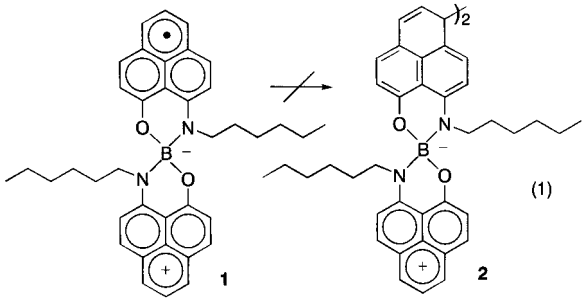

Nakasuji, has reported a sterically hindered phenalenyl derivative that exists as a π-dimer.[7] Solid-state dimerization is usually associated with a transition to an insulating ground state, but in the present paper we show that the conductivity in two new spiro-biphenalenyls increases on dimerization while the magnetic properties change from that of a paramagnetic free radical to a diamagnetic molecular crystal.

There are a number of difficulties in the realization of a molecular metal based on phenalenyl: (1) The strength of the carbon−carbon bond makes it difficult to suppress σ-dimerization (eq 1) [in the absence of steric factors].[7−12] (2) Like most

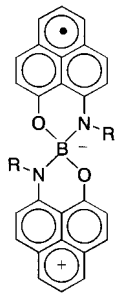

1, R =Hx
3, R =Et
4, R =Bu

delocalized organic radicals, phenalenyl is planar and therefore

* Author for correspondence. Present address: Departments of Chemistry and Chemical & Environmental Engineering, University of California, Riverside, CA 92521-0403.
[†] University of Kentucky.
[‡] University of Toledo.
[§] University of Waterloo.
[||] University of Arkansas.

(1) Haddon, R. C. *Nature* **1975**, *256*, 394−396.
(2) Haddon, R. C. *Aust. J. Chem* **1975**, *28*, 2343−2351.
(3) Haddon, R. C.; Wudl, F.; Kaplan, M. L.; Marshall, J. H.; Cais, R. E.; Bramwell, F. B. *J. Am. Chem. Soc.* **1978**, *100*, 7629−7633.
(4) Haddon, R. C.; Chichester, S. V.; Stein, S. M.; Marshall, J. H.; Mujsce, A. M. *J. Org. Chem.* **1987**, *52*, 711−712.
(5) Chi, X.; Itkis, M. E.; Patrick, B. O.; Barclay, T. M.; Reed, R. W.; Oakley, R. T.; Cordes, A. W.; Haddon, R. C. *J. Am. Chem. Soc.* **1999**, *121*, 10395−10402.
(6) Barclay, T. M.; Cordes, A. W.; Haddon, R. C.; Itkis, M. E.; Oakley, R. T.; Reed, R. W.; Zhang, H. *J. Am. Chem. Soc.* **1999**, *121*, 969−976.
(7) Goto, K.; Kubo, T.; Yamamoto, K.; Nakasuji, K.; Sato, K.; Shiomi, D.; Takui, T.; Kubota, M.; Kobayashi, T.; Yakusi, K.; Ouyang, J. *J. Am. Chem. Soc.* **1999**, *121*, 1619−1620.

10.1021/ja0039785 CCC: $20.00
Published on Web 04/06/2001

Scheme 1

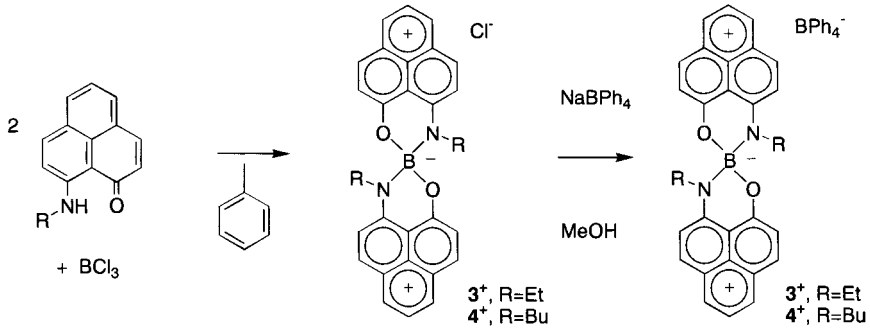

predisposed to the formation of one-dimensional stacks which are subject to electronic instabilities with insulating ground states (3) Radicals are usually expected to give rise to exactly half-filled bands, which are especially prone to charge density waves and a large on-site Coulombic correlation energy. As discussed previously,[5] the spiro-biphenalenyls circumvent most of these problems although it should be noted that these neutral carbon-based radicals are still free to undergo σ-dimerization (see refs 8 and 9) at a number of positions in the phenalenyl ring (eq 1). In the present paper we report the preparation, properties, and solid-state characterization of the ethyl (**3**) and butyl (**4**) derivatives of **1**; both of these compounds are found to be conducting π-dimers in the solid state, but with different room-temperature magnetic ground states.

Results and Discussion

Preparation and Solution Properties of Radicals 3 and 4. We prepared the ethyl and butyl variants of **1** via the chlorides ($\mathbf{3}^+$ Cl^- and $\mathbf{4}^+$ Cl^-), but finally employed the tetraphenylborate anion to obtain the required solubility properties for the salts (Scheme 1).

The electrochemistries of the salts $\mathbf{3}^+$ BPh_4^- and $\mathbf{4}^+$ BPh_4^- are presented in Figure 1, and it may be seen that both compounds show well-behaved reductions at potentials that are close to those seen for the salt of **1**.[5] The disproportionation potentials of $\Delta E^{2-1} = E_2^{1/2} - E_1^{1/2} = -0.35$ to -0.37 V, are quite low for all of these compounds. The ΔE^{2-1} value largely determines the on-site Coulombic correlation energy (U) in the solid state and is well-established as an important discriminator for organic metals.[13,14]

As before, we used cobaltocene as a reductant, because the oxidation potential ($E^{1/2} = -0.91$ V),[15] falls between the $E_1^{1/2}$ and $E_2^{1/2}$ reduction potentials of the salts.[5] For optimum crystal quality the H-cell must be loaded in a drybox and the solvent (acetonitrile) then rigorously degassed on a vacuum line before allowing the reagents to mix (Scheme 2).

X-ray Crystal Structures of 3 and 4. The structures of **3** and **4** were determined at 173 K (Figures 2 and 3), and in each case there are four molecules in the unit cell (two pairs of enantiomers). After we observed the anomalous magnetic and conductivity properties of these compounds (below), we also determined the structure of **3** at temperatures of 20, 100, and 293 K. The parameters for the structure determinations are reported in Table 1, and it may be seen that the structural changes in **3** over the full temperature range are extremely subtle.

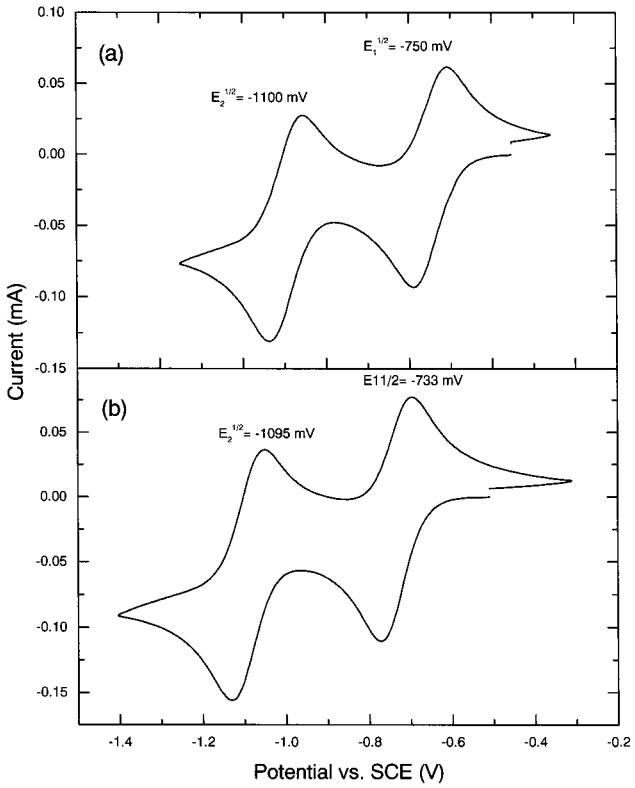

Figure 1. Cyclic voltammetry of (a) **3** and (b) **4**, in acetonitrile, referenced to SCE via internal ferrocence (not shown).

The stereoviews of the two radicals at 173 K (Figures 2 and 3), show that the compounds exist as π-dimers. The projection given in Figure 4 demonstrates the almost perfect superposition of the active carbon atoms in the π-dimers. Inspection of the singly occupied molecular orbital (SOMO) in the phenalenyl system shows that this configuration minimizes the steric interference while retaining the optimal overlap of the atoms that carry most of the spin density.[1,2] In the case of **3**, there is clear evidence for two types of π-dimers, and the distinction is apparent in the mean plane separations of the face-to-face dimer pairs (Figure 5). At low temperatures (20 and 100 K), the mean plane separations are 3.16 and 3.18 Å, whereas this parameter rises to 3.31 and 3.35 Å at temperatures of 173 and 293 K, respectively. On the basis of the magnetic data (below), we refer

(8) McBride, J. M. *Tetrahedron* **1974**, *30*, 2009−2022.
(9) Griller, D.; Ingold, K. U. *Acc. Chem. Res.* **1976**, *9*, 13−19.
(10) Ballester, M. *Acc. Chem. Res.* **1985**, *18*, 380−387.
(11) Sitzmann, H.; Bock, H.; Boese, R.; Dezember, T.; Havlas, Z.; Kaim, W.; Moscherosch, M.; Zanathy, L. *J. Am. Chem. Soc.* **1993**, *115*, 5, 12003−12009.
(12) Apeloig, Y.; Bravo-Zhivotskii, D.; Bendikov, M.; Danovich, D.; Botoshansky, M.; Vakul'skaya, T.; Voronokov, M.; Samoilova, R.; Zdravkova, M.; Igonin, V.; Shklover, V.; Struchkov, Y. *J. Am. Chem. Soc.* **1999**, *121*, 8118−8119.
(13) Garito, A. F.; Heeger, A. J. *Acc. Chem. Res.* **1974**, *7*, 232−240.
(14) Torrance, J. B. *Acc. Chem. Res.* **1979**, *12*, 79−86.
(15) Robbins, J. L.; Edelstein, L.; Spencer, B.; Smart, J. C. *J. Am. Chem. Soc.* **1982**, *104*, 1882−1893.

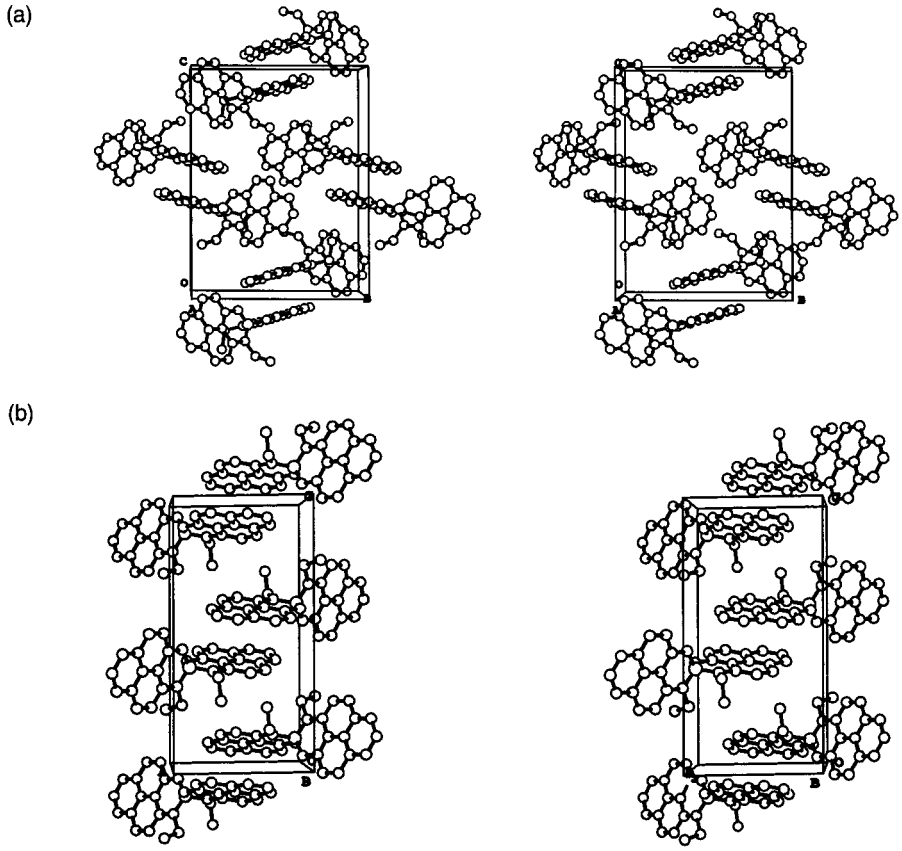

Figure 2. Stereoview of crystalline **3** viewed down: (a) the *x*-axis and (b) the *y*-axis.

Scheme 2

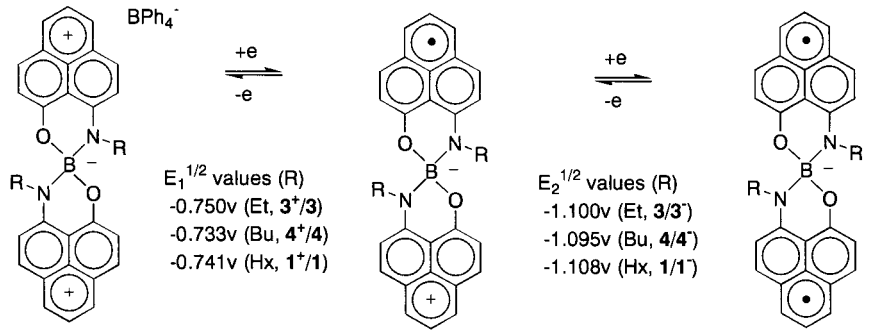

to these structures as the diamagnetic π-dimer (low-temperature form) and the paramagnetic π-dimer (high-temperature form). The structure of **4** (determined at 173 K), corresponds to a diamagnetic π-dimer (mean plane separation of 3.12 Å).

It seemed that the dimerization might be connected to the localization of the spin density at one of the phenalenyl units (cf. resonance structures drawn for **1**−**4** and Discussion in ref 5), with concomitant localization of a positive charge in the phenalenyl unit that forms the other component of the spiro linkage to the boron atom. Although the SOMO is largely nonbonding,[5,16] there are nonzero coefficients on some adjacent atoms, and thus it might be expected that population of this orbital would lead to changes in the bond lengths of some parts of the substituted phenalenyl nucleus (Table 2, Figure 6). In an effort to seek information on this point we calculated the standard deviations of the bond lengths in the two halves of the molecules on either side of the spiro-linkage, reasoning that localization of the spin and charge in the stronger low-temperature π-dimers would lead to a larger standard deviation between formally equivalent bonds than would be observed in the high-temperature structures. This expectation was not borne out, and it seems that the transition from the paramagnetic π-dimer to the diamagnetic π-dimer does not exert a large effect on the molecular structure.

The structures of **3** and **4** stand in marked contrast to that of **1**, in which there is no evidence of σ- or π-dimerization over the full temperature range (4−400 K).[5] In a number of other respects, however, the structures are similar. Although there are π-dimers in **3** and **4**, the distances between the dimeric units still lie outside the sum of the van der Waals distances for the carbon atoms (3.4 Å, see Figure 7), just as the contacts between monomers of **1** were outside the sum of the van der Waals separations for carbon atoms. Thus, it could be argued that in all of these compounds the lattice building blocks—whether monomer or dimer—are isolated in the crystal lattice, with no close contacts or long-range stacking, and it appears that the molecules (or dimers) sit in the lattice completely independent of one another.

(16) Haddon, R. C.; Chichester, S. V.; Marshall, J. H. *Tetrahedron* **1986**, *42*, 6293−6300.

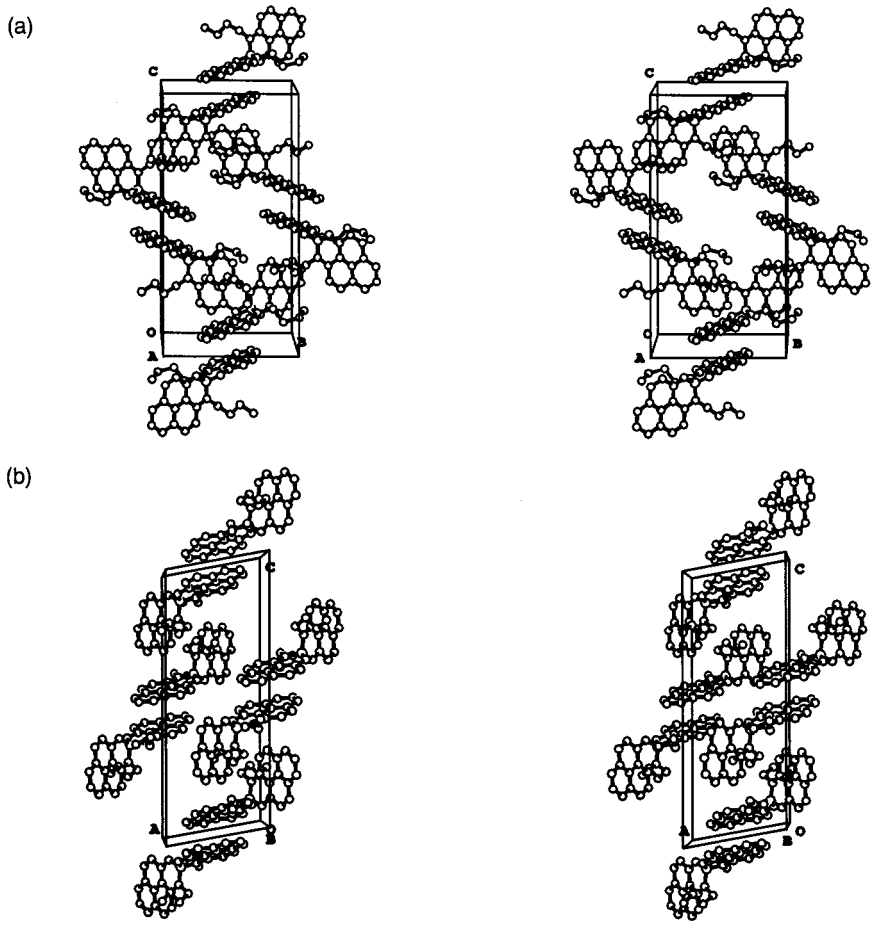

Figure 3. Stereoview of crystalline **4** viewed down: (a) the *x*-axis and (b) the *y*-axis.

Table 1. Crystal Data for **3** and **4**

compd	**3**				**4**
formula	$C_{30}H_{24}BN_2O_2$				$C_{34}H_{32}BN_2O_2$
fw	455.3				511.4
space group	$P2_1/c$				$P2_1/n$
Z	4				4
μ, mm^{-1}	0.08				0.08
temp, K	20(2)	100(1)	173(2)	293(1)	173(2)
a (Å)	9.0240(2)	9.0680(7)	9.044(1)	9.1253(4)	8.962(1)
b (Å)	13.5725(1)	13.6008(10)	13.572(1)	13.5747(6)	12.161(1)
c (Å)	17.7556(4)	17.8547(10)	18.082(2)	18.2219(8)	23.642(2)
β (deg)	90.6348(12)	90.684(3)	91.12(1)	90.688(1)	100.88(1)
V (Å^3)	2174.54(7)	2201.9(3)	2219.1(4)	2257.04(17)	2530.4(4)
θ(max) (deg)	29.9	29.8	25.0	29.9	25.0
refine data(all)	5750	5888	3625	6063	4595
params refined	412	412	412	412	480
$R(F)$, $R_w(F^2)$	0.094, 0.165	0.105, 0.122	0.158, 0.150	0.145, 0.112	0.095, 0.107
$R(F)(F^2 > 2\sigma)$	0.055	0.051	0.064	0.045	0.047
mean plane separations (Å)	3.16	3.18	3.31	3.35	3.12

Solid State Properties of 3 and 4. We measured the magnetic susceptibilities (χ), of **3** and **4** over temperature (T) ranges of 4 to room temperature and 4−400 K, using a Faraday balance. At low temperatures (T < 100 K), both compounds show Curie behavior due to a small amount of paramagnetic defects in the lattice (Figures 8a and 9a), but in this temperature regime we consider the compounds to exist as diamagnetic π-dimers. At higher temperatures both compounds undergo dissociation to free radicals in which essentially all of the coupled spins unpair and the Curie spin count[5] approaches unity, and we refer to these structures as paramagnetic π-dimers.

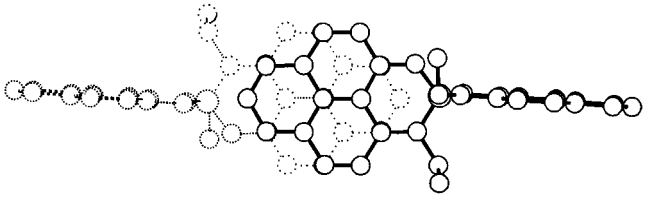

Figure 4. Overlap between one pair of enantiomers of crystalline **3** (173 K).

Electrical resistivity (ρ) measurements of single crystals of **3** and **4** (along the a^* axes), were conducted over the same

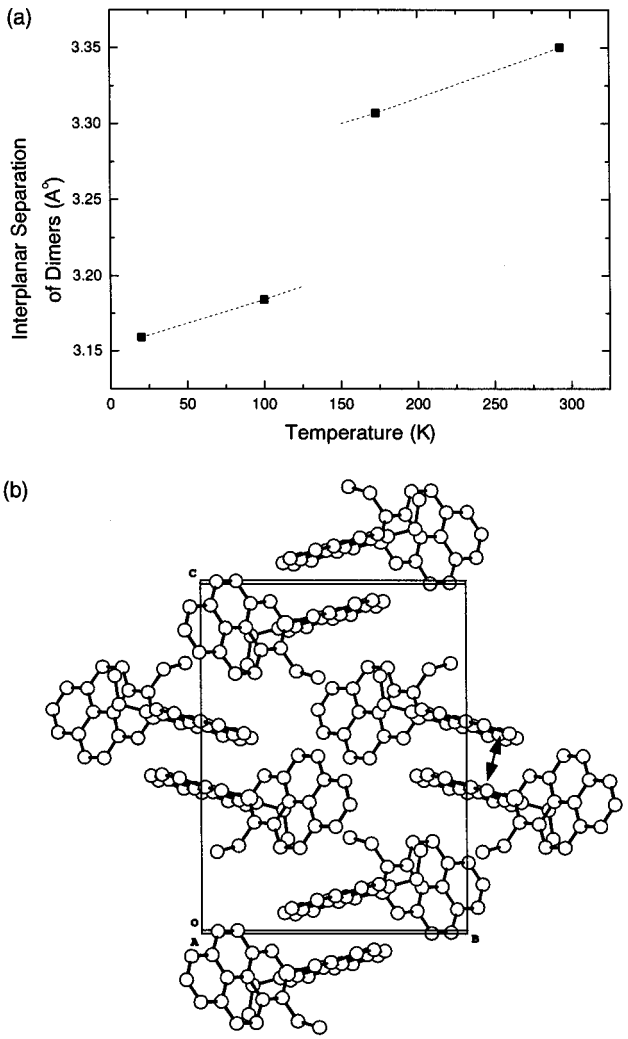

Figure 5. (a) Distance between the parallel planes of pairs of enantiomers as a function of temperature and (b) diagram showing the distance between the planes in the crystal lattice.

temperature range that was employed for the magnetic studies (Figures 8 and 9). In both cases the transition from the high-temperature paramagnetic π-dimer form to the low-temperature diamagnetic π-dimer structure is accompanied by an increase in conductivity (σ) by about 2 orders of magnitude. This behavior is unprecedented and is very difficult to reconcile with the usual understanding of a Peierls dimerization, which inevitably leads to an insulating ground state.[13,14]

Band Electronic Structure of 3 and 4. The maximum conductivities measured for crystals of **1**, **3**, and **4** are the highest yet seen for neutral molecular conductors,[6] and these values are very difficult to reconcile with the solid-state packing and the measured magnetic susceptibility which provide no evidence for a conducting pathway in the lattice. The additional unusual feature provided by **3** and **4** is the presence of π-dimers in the lattice, and the increased conductivity as the dimerization strengthens and pairs the electrons.

In an effort to throw further light on these questions, we carried out extended Hückel theory (EHT) band structure calculations[17] on the crystal structure. Such calculations have been very useful in understanding the electronic structure of the organic molecular superconductors[18] and thin-film field effect transistors[19] but cannot be expected to succeed in situations where the tight-binding approximation is not applicable; our previous experience with **1** suggests that the results obtained by application of tight-binding theory to these radicals must be viewed with caution.

The results are shown in Figure 10 for band structure calculations carried out on the lattices found in the X-ray crystal structures. The eight bands shown in Figure 10 are derived from the two LUMOs of $\mathbf{3}^+$ ($\mathbf{4}^+$) for each of the four molecules of **3** (**4**) in the unit cell; these basically consist of the symmetric and antisymmetric combinations of the 1,9-disubstituted-phenalenyl LUMO.[5,16] Alternatively, they can be viewed as arising from the nonbonding molecular orbitals[1,2] of each of the eight phenalenyl units in the unit cell. In a band picture these eight orbitals now accommodate a total of four electrons, leading to a one-fourth-filled band complex with two filled and six vacant bands. The tight binding picture fails, of course, because the magnetic susceptibility shows that the electrons are unpaired in compound **3** at 173 K (Figure 10a). The calculations do show the large increase in the gap between the 2 lowest orbitals and the remainder of the band complex as the temperature decreases from 173 to 100 K in **3** (transition from a paramagnetic π-dimer to a diamagnetic π-dimer as the four electrons pair up in these two low-lying orbitals); the energy gap increases from about 0.2 to 0.5 eV below the transition. As expected, the band structures of **3** at 100 K and **4** at 173 K are similar, because both are diamagnetic π-dimers under these conditions. The band structures show the same relatively small dispersions found in **1**. In **1** the maximum dispersion found in any band was 0.075 eV, whereas the 100 K structure of **3** shows a dispersion of 0.15 eV in one of the conduction bands. The properties of the diamagnetic π-dimer state of **3** at 100 K are even more difficult to rationalize than the behavior that we found for **1**.[5] Compound **1** was shown to exhibit Curie paramagnetism over essentially the whole temperature range (no dimerization) with activated conductivity that was fit with a mobility model.[20] In this mobility model,[20] the number of carriers (n_c) and the mobility are both temperature-dependent, and the conductivity is given by $\sigma(T) = n_c(T)e\mu(T)$, where $n_c(T) = n \exp(\Delta/kT)$ and $\mu(T) = AT^{-\alpha}$. A fit of this function gave $\alpha = 5.5$, $E_g = 2\Delta = 0.4$ eV, $\mu(T = 300\ \text{K}) = 0.4\ \text{cm}^2/\text{Vs}$ and $\mu(T = 100\ \text{K}) = 170\ \text{cm}^2/\text{Vs}$.[5] The strong temperature dependence in the mobility originates from the scattering by optical phonons (molecular vibrations). The relevant energy gap (Δ), is simply given by $\Delta = U$, the on-site Coulombic correlation energy. Thus, the transport properties of crystalline **1** arise from thermal population of the conduction band. The ground state is localized, and thus leads to Curie behavior in the measured magnetic susceptibility. To a first approximation we suggested that crystalline **1** should be viewed as a degenerate Mott−Hubbard insulator with a small value of U and a surprisingly broad conduction band.[5]

In the high-temperature state (paramagnetic π-dimer) of **3** and **4**, the properties resemble those found for **1**, although the dimerization present in the lattice of **3** and **4**, even at these temperatures, serves to significantly spread the total bandwidth to about 1 eV, as compared with 0.31 eV in **1**. At 100 K, spin-pairing in **3** is virtually complete, and from the magnetic and structural point of view, **3** is best described as a diamagnetic π-dimer in this temperature regime. We have studied a number of such (stacked) sulfur−nitrogen diamagnetic π-dimers, and

(17) Hofmann, R. *Solids and Surfaces*; VCH: New York, 1988.

(18) Haddon, R. C.; Ramirez, A. P.; Glarum, S. H. *Adv. Mater.* **1994**, *6*, 316−322.

(19) Haddon, R. C.; Siegrist, T.; Fleming, R. M.; Bridenbaugh, P. M.; Laudise, R. A. *J. Mater. Chem* **1995**, *5*, 1719−1724.

(20) Epstein, A. J.; Conwell, E. M.; Miller, J. S. *Ann. N. Y. Acad. Sci.* **1978**, *313*, 183−209.

Table 2. Bond Lengths and the Interplanar Separation (*D*) of the Interdimer Planes of **3** as a Function of Temperature

T	20 K	100 K	173 K	293 K	*T*	20 K	100 K	173 K	293 K
D	3.159	3.184	3.307	3.35	*D*	3.159	3.184	3.307	3.35
C1−C2	1.404(2)	1.405(2)	1.419(4)	1.410(2)	B−N2	1.546(2)	1.553(2)	1.510(4)	1.516(2)
C2−C3	1.377(3)	1.377(2)	1.361(4)	1.366(3)	B−O2	1.487(2)	1.486(2)	1.456(4)	1.457(2)
C3−C3a	1.414(3)	1.421(2)	1.417(4)	1.412(3)	N2−C19	1.351(2)	1.352(2)	1.368(3)	1.375(2)
C3a−C4	1.414(2)	1.414(2)	1.404(4)	1.406(3)	O2−C11	1.329(2)	1.3349(19)	1.352(3)	1.351(2)
C4−C5	1.383(3)	1.382(2)	1.380(4)	1.374(3)	C11−C12	1.416(3)	1.412(2)	1.396(4)	1.394(2)
C5−C6	1.389(3)	1.391(2)	1.392(4)	1.383(3)	C12−C13	1.366(3)	1.367(2)	1.372(4)	1.365(2)
C6−C6a	1.407(2)	1.411(2)	1.398(4)	1.396(2)	C13−C13a	1.426(3)	1.428(2)	1.423(4)	1.411(3)
C6a−C7	1.425(2)	1.423(2)	1.428(4)	1.426(2)	C13a−C14	1.416(3)	1.419(2)	1.421(4)	1.418(3)
C7−C8	1.372(2)	1.377(2)	1.349(4)	1.352(3)	C14−C15	1.384(3)	1.390(3)	1.390(5)	1.379(3)
C8−C9	1.421(2)	1.425(2)	1.436(4)	1.433(2)	C15−C16	1.389(3)	1.386(3)	1.377(5)	1.377(3)
C9−C9a	1.441(2)	1.436(2)	1.431(4)	1.438(2)	C16−C16a	1.403(2)	1.407(2)	1.409(4)	1.414(3)
C9a−C1	1.403(2)	1.411(2)	1.400(3)	1.398(2)	C16a−C17	1.425(3)	1.431(2)	1.405(4)	1.410(2)
C9a−C9b	1.424(2)	1.427(2)	1.425(3)	1.421(2)	C17−C18	1.361(3)	1.362(2)	1.365(4)	1.368(3)
C9b−C3a	1.429(2)	1.428(2)	1.418(4)	1.414(2)	C18−C19	1.434(3)	1.437(2)	1.415(4)	1.413(2)
C9b−C6a	1.424(2)	1.428(2)	1.417(3)	1.416(2)	C19−C19a	1.436(2)	1.438(2)	1.429(4)	1.425(2)
C1−O1	1.346(2)	1.3524(19)	1.334(3)	1.3320(19)	C19a−C11	1.404(2)	1.413(2)	1.413(4)	1.408(2)
O1−B	1.452(2)	1.455(2)	1.476(4)	1.478(2)	C19a−C19b	1.427(2)	1.428(2)	1.415(4)	1.425(2)
C9−N1	1.363(2)	1.365(2)	1.333(3)	1.333(2)	C19b−C13a	1.421(3)	1.423(2)	1.420(4)	1.417(2)
N1−B	1.524(2)	1.526(2)	1.559(3)	1.552(2)	C19b−C16a	1.423(3)	1.426(2)	1.431(4)	1.422(2)

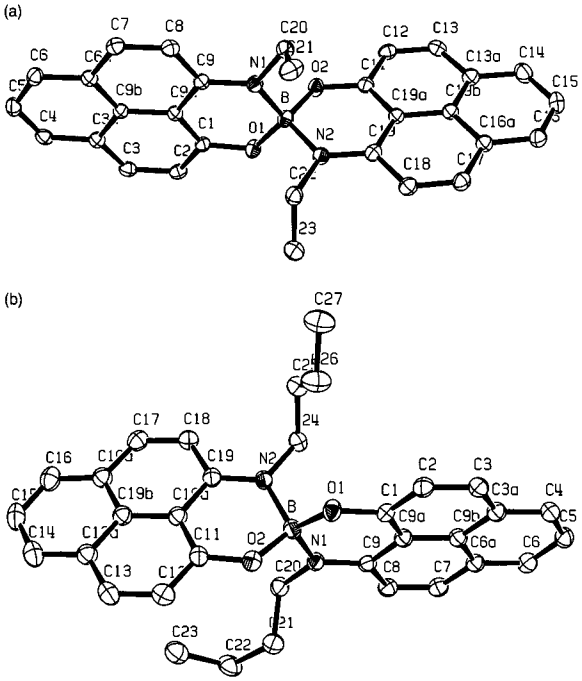

Figure 6. ORTEP diagram of the molecular structure of **3** and **4** and the numbering of the atoms.

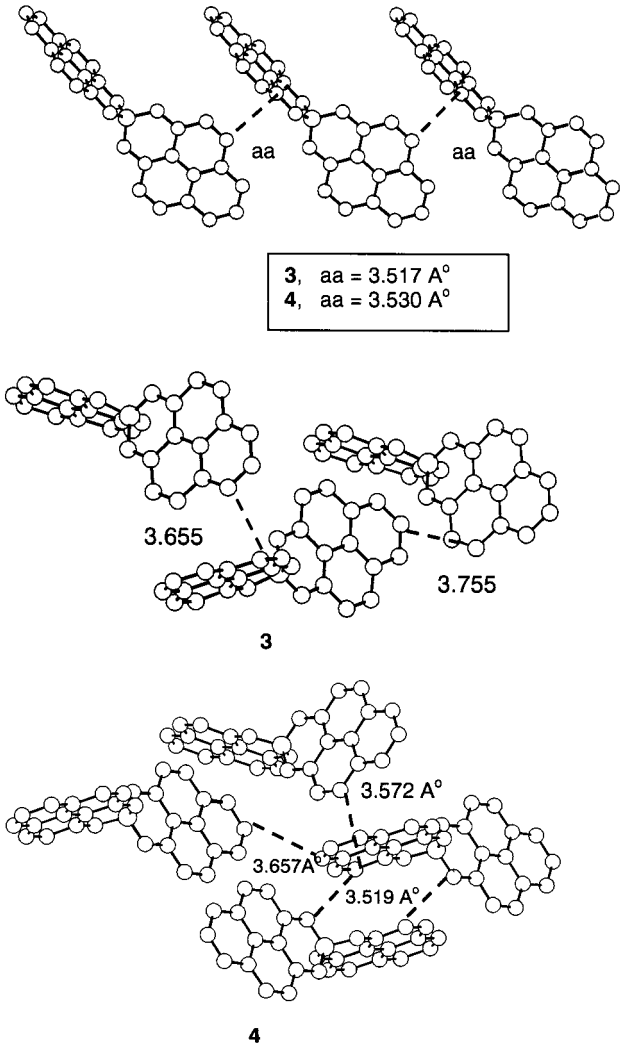

Figure 7. Closest non-dimer intermolecular C···C contacts between phenalenyl units in the crystal lattice of **3** and **4**.

they are invariably insulating.[21] We tentatively assign the enhancement in the conductivity at 100 K, to a decrease in the on-site Coulombic correlation energy (*U*), as the dimers form a super-molecule with twice the amount of conjugation. This interpretation is supported by fits to the conductivity data of **3** (not shown), above and below the transition at 100 K. In the high-temperature regime ($T > 100$ K, paramagnetic π-dimer), the (conductivity) energy gap is $E_g = 2\Delta = 0.23$ eV, whereas it falls to $E_g = 2\Delta = 0.1$ eV below the transition ($T < 100$ K, diamagnetic π-dimer). The enhanced conductivity at the phase transition could be associated with the band crossings that occur along a* (the axis of the conductivity measurements), at the phase transition (see Figure 10a,b).

Conclusions

The properties of the spiro-biphenalenyls continue to challenge our understanding of conducting organic molecular crystals,[5] and further work will be necessary to rationalize their behavior. The finding that dimerization in crystalline **3** and **4** enhances conductivity is unprecedented and further emphasizes

(21) Oakley, R. T. *Can. J. Chem.* **1993**, *71*, 1775−1784.

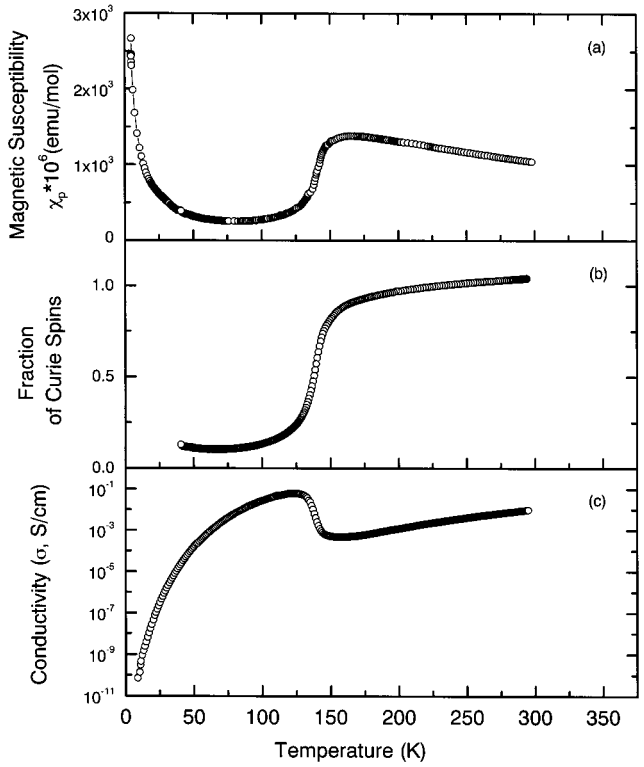

Figure 8. (a) Magnetic susceptibility, (b) fraction of Cure spins, and (c) single-crystal conductivity of **3** as a function of temperature.

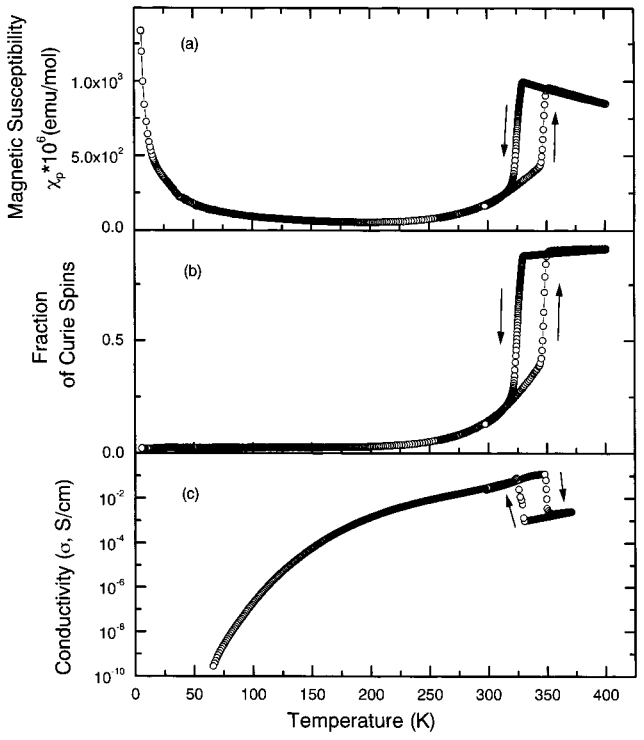

Figure 9. (a) Magnetic susceptibility, (b) fraction of Cure spins and (c) single-crystal conductivity of **4** as a function of temperature.

the point that magnetism, resistivity, structure, and band structure are not well-correlated in these organic solids.

Experimental Section

Materials. Boron trichloride (Aldrich), sodium tetraphenylborate (Aldrich), and cobaltocene (Strem) were all commercial products and were used as received. 9-Hydroxy-1-oxophenalene was synthesized according to literature procedures.[22] Toluene was distilled from sodium benzophenone ketyl immediately before use. Acetonitrile was distilled from P_2O_5 and then redistilled from K_2CO_3 immediately before use.

9-*N*-Ethylamino-1-oxo-phenalene. A mixture of 9-hydroxy-1-oxophenalene (1.96 g, 0.01 mol) and aqueous ethylamine (20 mL, 70% solution) was placed in a heavy-walled sealed tube with an Ace thread at one end and sealed with a Teflon plug. The glass tube and plug are available from Ace Glass Inc., Vineland, NJ. The contents were stirred at a temperature of 125 °C for 2 h. The mixture was allowed to cool, the tube was vented and opened, and the contents were poured into 100 mL of distilled water. The aqueous mixture was extracted with benzene, and the organic layer was separated, dried with magnesium sulfate, and taken down on a rotary evaporator to give a brownish-yellow oil. Crystallization from hexane gave red plates. Yield: 1.85 g (82%); mp 61 °C. ^{1}H NMR (CD_3CN): δ 12.05 (b, 1H), 8.00 (d, 1H), 7.83−7.94 (m, 3H), 7.41 (t, 1H), 7.24 (d, 1H), 6.83 (d, 1H), 3.54 (d of q, 2H), 1.37 (t, 3H). Anal. Calcd for $C_{15}H_{13}ON$: C, 80.69; H, 5.87; N, 6.27. Found: C, 81.03; H, 5.87; N, 6.47.

9-*N*-Butylamino-1-oxo-phenalene. A mixture of 9-hydroxy-1-oxophenalene (0.98 g, 0.005 mol) and butylamine (10 mL) was refluxed for 20 h in Ar. After cooling, yellow crystals formed. The resulting crystals were separated by filtration and purified by column chromatography on Al_2O_3 with $CHCl_3$ to give a red oil which solidified to a yellow solid (1.2 g, 94%); leaflets from heptane, mp 67 °C. ^{1}H NMR (CD_3CN): δ 12.23 (b, 1H), 8.07 (d, 1H), 7.88−7.98 (m, 3H), 7.45 (t, 1H), 7.33 (d, 1H), 6.85 (d, 1H), 3.57 (d of t, 2H), 1.63−1.83 (m, 2H), 1.42−1.60 (m, 2H), 1.00 (t, 3H). Calcd for $C_{17}H_{17}ON$: C, 81.24; H, 6.82; N, 5.57. Found: C, 81.31; H, 6.82; N, 5.66.

Preparation of 3^+, Cl^-. 9-*N*-Ethylamino-1-oxo-phenalene (1.2 g, 0.005 mol) in toluene (100 mL) was treated with boron trichloride in dichloromethane (2.2 mL, 0.0022 mol) under argon in the dark, and the mixture was refluxed overnight. The yellow solid was isolated by filtration (1.03 g, 90%). IR (HART, 1700−690 cm^{-1}): 1626 (m), 1595 (w), 1585 (m), 1574 (m), 1516 (s), 1493 (w), 1472 (w), 1448 (w), 1392 (m), 1364 (w), 1346 (w), 1328 (w), 1299 (s), 1249 (m), 1230 (w), 1197 (w), 1163 (m), 1142 (w), 1135 (m), 1108 (w), 1081 (w), 1047 (w), 1027 (s), 1001 (w), 952 (m), 862 (m), 823 (m), 806 (m), 788 (w), 768 (w), 731 (w), 709 (w), 696 (w).

Preparation of 4^+, Cl^-. 9-*N*-Butylamino-1-oxo-phenalene (1.4 g, 0.0056 mol) in toluene (100 mL) was treated with boron trichloride in dichloromethane (2.7 mL, 0.0027 mol) under argon in the dark, and the mixture was refluxed overnight. The yellow solid was isolated by filtration (1.72 g, 93%). IR (HART, 1700−690 cm^{-1}): 1627 (m), 1586 (m), 1571 (m), 1515 (s), 1490 (w), 1472 (w), 1447 (w), 1395 (m), 1359 (m), 1296 (s), 1249 (m), 1236 (w), 1225 (w), 1201 (m), 1172 (m), 1144 (m), 1133 (m), 1111 (w), 1102 (w), 1051 (w), 1032 (s), 1007 (w), 960 (w), 933 (m), 883 (m), 863 (m), 847 (w), 824 (w), 784 (w), 762 (m), 751 (w), 710 (w).

Preparation of 3^+, BPh_4^-. A solution of 0.5 g of Na BPh_4 in 10 mL of MeOH was added to a solution of 3^+, Cl^-, (0.5 g) in 40 mL of MeOH. A yellow precipitate formed immediately. The mixture was stirred for 5 min, and 0.4 g (51%) of yellow solid was separated by filtration and stored in the dark. The yellow product was purified by crystallization from a dichloromethane/methanol mixture. ^{1}H NMR (CD_3CN): δ 8.51 (d, 2H), 8.45 (d, 2H), 8.32 (m, 4H), 7.81 (t, 2H), 7.47 (m, 4H), 7.25 (b, 8H), 6.98 (t, 8H), 6.82 (t, 4H), 3.74 (b, 2H), 3.48 (b, 2H), 1.27 (t, 6H). IR (4000−400 cm^{-1}): ν = 3056 (m), 3033 (m), 2955 (m) 2926 (m), 2855 (m), 1951 (w), 1628 (s), 1585 (s), 1573 (s), 1585 (s), 1515 (s), 1470 (m), 1446 (m), 1425 (w), 1413 (w), 1389 (m), 1357 (m), 1333 (w), 1294 (s), 1244 (m), 1190 (m), 1166 (m), 1136 (m), 1100 (w), 1040 (m), 1016 (m), 963 (w), 903 (w), 879 (w), 845 (m), 824 (w), 769 (w), 731 (m), 706 (m), 612 (w), 580 (w), 549 (w), 494 (w). Anal. Calcd for $C_{54}H_{44}O_2N_2B_2$: C, 83.74; H, 5.73; N, 3.62; B, 2.79. Found: C, 84.07; H, 5.71; N, 3.82; B, 2.86.

Preparation of 4^+, BPh_4^-. A solution of 0.52 g of Na BPh_4 in 20 mL of MeOH was added to a solution of 4^+, Cl^-, (0.5 g) in 50 mL of MeOH. A yellow precipitate formed immediately. The mixture was stirred for 5 min, and 0.68 g (85%) of yellow solid was separated by

(22) Haddon, R. C.; Chichester, S. V.; Mayo, S. L. *Synthesis* **1985**, 639−641.

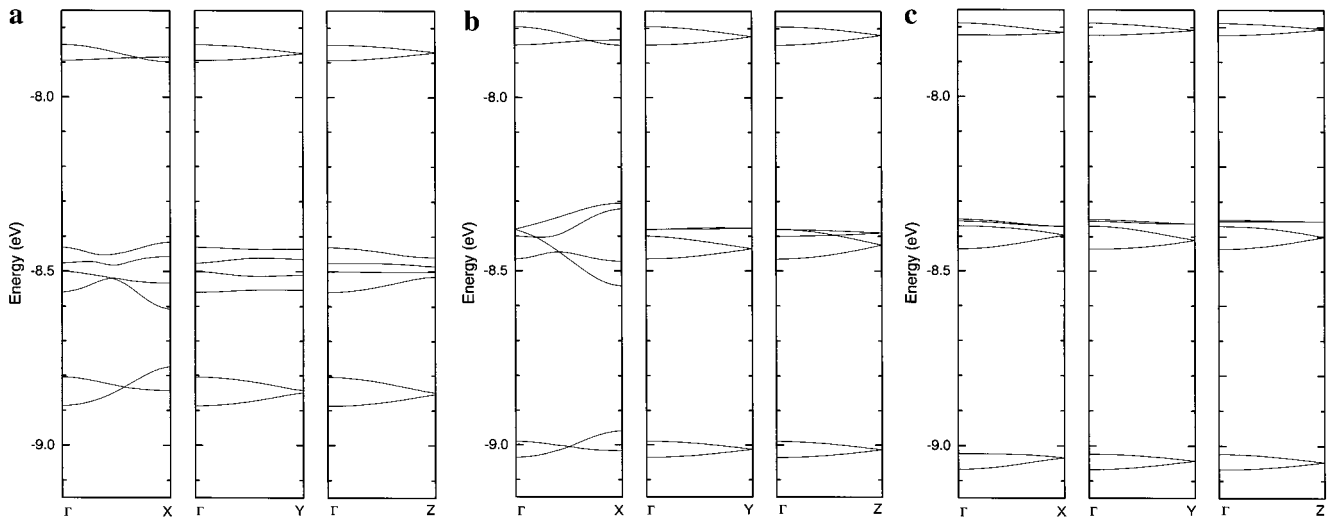

Figure 10. Calculated band structures of (a) crystalline **3** at 173 K, (b) crystalline **3** at 100 K, and (c) crystalline **4** at 173 K.

filtration and stored in the dark. The yellow product can be purified by recrystallization from an acetonitrile/methanol mixture. ^{1}H NMR (CD_3CN): δ 8.54 (d, 2H), 8.43 (d, 2H), 8.33 (m, 4H), 7.83 (t, 2H), 7.46 (m, 4H), 7.25 (m, 8H), 6.97 (t, 8H), 6.82 (t, 4H), 3.66 (b, 2H), 3.30 (b, 2H), 1.72 (b, 4H), 1.18 (b, 4H), 0.67 (t, 6H). IR (4000−400 cm^{-1}): ν = 3056 (m), 3033 (m), 2955 (m) 2926 (m), 2855 (m), 1951 (w), 1628 (s), 1585 (s), 1573 (s), 1585 (s), 1515 (s), 1470 (m), 1446 (m), 1425 (w), 1413 (w), 1389 (m), 1357 (m), 1333 (w), 1294 (s), 1244 (m), 1190 (m), 1166 (m), 1136 (m), 1100 (w), 1040 (m), 1016 (m), 963 (w), 903 (w), 879 (w), 845 (m), 824 (w), 769 (w), 731 (m), 706 (m), 612 (w), 580 (w), 549 (w), 494 (w). Anal. Calcd for $C_{58}H_{52}O_2N_2B_2$: C, 83.86; H, 6.31; N, 3.37; B, 2.60. Found: C, 83.75; H, 6.32; N, 2.98; B, 2.31.

Crystallization of 3. An invertable H-Cell with a glass D frit was loaded in a drybox. A solution of 150 mg of $\mathbf{3}^+$, BPh_4^- in 20 mL of dry CH_3CN was placed in one container, and 40 mg of $CoCp_2$ dissolved in 20 mL of dry CH_3CN in the other container. The containers were attached to the inverted H-cell in the drybox. The H-cell is removed from the drybox and attached to a vacuum line, and the containers were taken through three cycles of freeze, pump, and thaw to degas the solutions. The H-cell was inverted, and the solutions were allowed to diffuse through the glass frit. After sitting in the dark for 1 week the cell yielded 50 mg of black shinning blades. IR(HART, 4000−680 cm^{-1}): 2954 (m), 2927 (m), 2855 (m), 1626 (m), 1586 (w), 1565 (s), 1536 (w), 1510 (m), 1487 (vw), 1465 (m), 1442 (m), 1414 (vw), 1389 (w), 1350 (m), 1331 (m), 1287 (s), 1238 (s), 1191 (m), 1156 (m), 1136 (m), 1112 (w), 1099 (w), 1065 (m), 1056 (m), 1037 (m), 1008 (m), 990 (s), 965 (m), 935 (m), 910 (w), 879 (m), 848 (m), 831 (m), 811 (w), 789 (vw), 771 (m), 760 (m), 754 (m), 723 (w), 716 (w), 695 (m), 682(m). Anal. Calcd for $C_{30}H_{24}O_2N_2B$: C, 79.13; H, 5.31; N, 6.15; B, 2.31. Found: C, 78.93; H, 5.34; N, 6.30; B, 2.26.

Crystallization of 4. An invertable H-Cell with a glass D frit was loaded in a drybox. A solution of 130 mg of $\mathbf{4}^+$, BPh_4^- in 20 mL of dry CH_3CN was placed in one container, and 33 mg of $CoCp_2$ was dissolved in 20 mL of dry CH_3CN in the other container. The containers were attached to the inverted H-cell in the drybox. The H-cell was removed from the drybox and attached to a vacuum line, and the containers were taken through three cycles of freeze, pump, and thaw to degas the solutions. The H-cell was inverted, and the solutions were allowed to diffuse through the glass frit. After sitting in the dark for 1 week the cell yielded 24 mg of black shinning needles. IR(HART, 4000−680 cm^{-1}): 2954 (m), 2927 (m), 2855 (m), 1626 (m), 1586 (w), 1565 (s), 1536 (w), 1510 (m), 1487 (vw), 1465 (m), 1442 (m), 1414 (vw), 1389 (w), 1350 (m), 1331 (m), 1287 (s), 1238 (s), 1191 (m), 1156 (m), 1136 (m), 1112 (w), 1099 (w), 1065 (m), 1056 (m), 1037 (m), 1008 (m), 990 (s), 965 (m), 935 (m), 910 (w), 879 (m), 848 (m), 831 (m), 811 (w), 789 (vw), 771 (m), 760 (m), 754 (m), 723 (w), 716 (w), 695 (m), 682(m). Anal. Calcd for $C_{34}H_{32}O_2N_2B$: C, 79.85; H, 6.31; N, 5.48; B, 2.11. Found: C, 79.86; H, 6.11; N, 5.72; B, 1.99.

X-ray Crystallography. All data were collected with Mo Kα radiation using diffractometers with CCD detectors. The data for the crystals of **3** at 293, 100, and 20 K were collected at the University of Toledo, using a Siemens SMART unit; the 173 K data for the crystals of **3** and **4** were collected at the University of Kentucky, using a Nonius KappaCCD system. The structures were solved by direct methods and in all cases the final Shelxl least-squares refinement (on Fsqd) included all data and isotropic refinement of the H atoms.

Magnetic Susceptibility Measurements The magnetic susceptibilities of **3** and **4** were measured over the temperature range of 5 to about 400 K on a George Associates Faraday balance operating at 0.5 T.

Conductivity Measurements. The single-crystal conductivity, σ, of **3** and **4** were measured in a four-probe configuration. The in-line contacts were made with silver paint. The samples were placed on a sapphire substrate, and electrical connections between the silver paint contacts and substrate were made by thin, flexible 25 μm diameter silver wires to relieve mechanical stress during thermal cycling of the sample. The conductivities were measured along the long axis of the crystals which were determined to correspond to the *a** direction during the X-ray crystallography studies.

Conductivity was measured in a custom-made helium variable-temperature probe using a Lake Shore 340 temperature controller. A Keithley 236 unit was used as a voltage source and current meter, and two 6517A Keithley electrometers were used to measure the voltage drop between the potential leads in a four-probe configuration.

Band Structure Calculations. The band structure calculations made use of a modified version of the extended Hückel theory (EHT) band structure program supplied by M.-H. Whangbo. The parameter set was chosen to provide a reasonably consistent picture of bonding in heterocyclic organic compounds.[19,23]

Acknowledgment. This work was supported by the Office of Basic Energy Sciences, Department of Energy under Grant No. DE-FG02-97ER45668.

JA0039785

(23) Cordes, A. W.; Haddon, R. C.; Oakley, R. T.; Schneemeyer, L. F.; Waszczak, J. V.; Young, K. M.; Zimmerman, N. M. *J. Am. Chem. Soc.* **1991**, *113*, 582.